Chem. Eng. Comm., 1996, Vols. 141–142, pp. 331–346
Reprints available directly from the publisher
Photocopying permitted by license only

DISPERSED FLOW HEAT TRANSFER IN CIRCULAR BENDS

M. J. WANG[1] and F. MAYINGER

Lehrstuhl A für Thermodynamik, Technische Universität München, 80290 München, Germany

(Received in final form April 19, 1995)

This paper presents an experimental study of dispersed flow heat transfer in 90-degree circular bends. From extensive measurements, two different heat transfer patterns are identified, i.e. heat transfer without and with rewetting. Their intrinsic mechanisms are analysed, based on the present experimental evidence and our previous theoretical studies. Effects of mass flow rate, wall heat flux, system pressure and curvature ratio on heat transfer are also investigated. An empirical criterion is developed to identify the heat transfer pattern in the bend.

KEYWORDS **Bend Dispersed flow Droplet dynamics Heat transfer**

INTRODUCTION

Dispersed flow heat transfer has been the subject of research for dozens of years because of its importance in many industrial applications, e.g. in the design and operating of the once-through steam generators and in the accident analysis of nuclear reactors. By dispersed flow, it is referred to the two-phase flow regime characterized by liquid droplets in dispersed form entrained in a continuous flowing vapor. Basically, heat is transferred in this flow regime from the wall by the following paths:

- Bulk and local vapor convection
- Dry and/or wet collisions of droplets on the wall
- Radiation to vapor and droplets.

In straight channels, numerous studies (Mayinger, 1982) indicate that vapor convection plays a dominant role to the wall heat transfer. Droplet collisions are of secondary importance, and radiation heat transfer can be neglected as long as the wall temperature is not extremely high.

When dispersed flow passes through a curved channel – a common geometry in practice, heat transfer mechanism may differ significantly to that in simple channels. The radially outward centrifugal forces and the gravitational forces produce phase separation in different directions. In addition, the imbalance between the pressure forces and the centrifugal forces induces a cross-stream secondary flow, superimposed on the primary flow (see Fig. 1). The secondary flow improves the vapor convection and brings about circumferential motions of liquid phase, especially the small droplets

[1] Current address: RUD. OTTO MEYER, 22339 Hamburg, Germany.

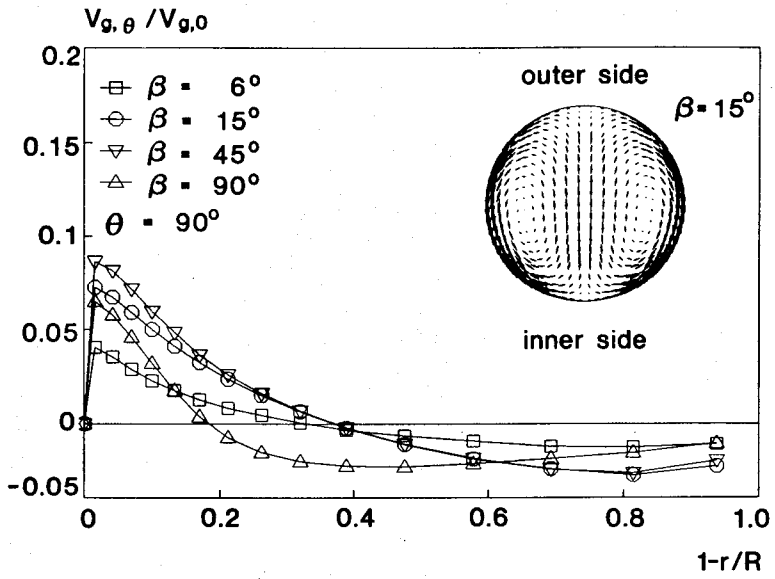

FIGURE 1 Secondary vapor flow at $R_c/R = 42$, $Re_g = 1.07 \times 10^6$, see Figure 3 for toroidal coordinate system (Wang and Mayinger, 1995).

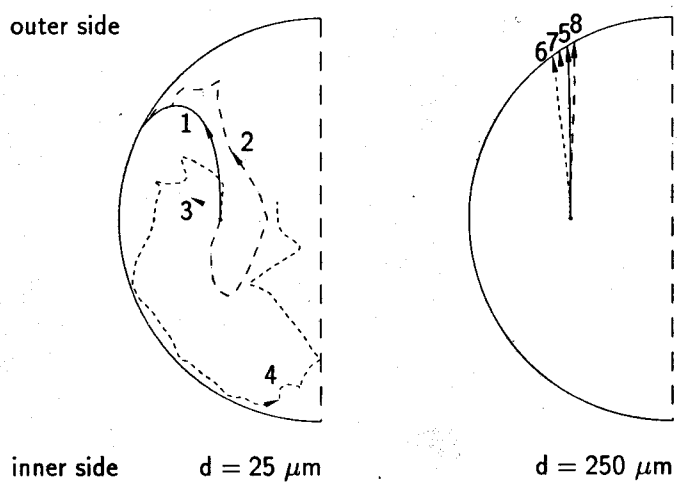

FIGURE 2 Droplet trajectories in the bend: $R_c/R = 42$, $Re_g = 1.07 \times 10^6$ (Wang and Mayinger, 1995).

(see Fig. 2). All these fluid-dynamic effects lead to exceptionally complicated heat transfer scenarios in curved channels.

Previous investigations on dispersed flow heat transfer in curved channels were mainly carried out in helical coils at high vapor qualities (e.g. Cumo *et al.*, 1972; Styrikovich *et al.*, 1984). In these experiments, heat transfer coefficient was found to be

higher than that in straight tubes due to the aforementioned fluid-dynamic changes. Because of the dominant centrifugal separation along the flow channel, wall temperature maintains highest value at the internal and lowest value at the external side of the coil. The temperature difference between these two extreme sides decreases with increases in pressure, vapor quality and mass flow rate. Lautenschlager (1988) studied dispersed flow heat transfer in 90-degree circular bends experimentally. Different from the previous observations, he found that under certain conditions, continuous vapor film on the wall could be interrupted by droplet impingement and rewetting on the bend wall may occur on the outside and then spread gradually over the whole circumference, resulting in the heat transfer augmentation. Due to the limited information on fluid dynamics, however, detailed analysis of heat transfer was not possible at that time.

Recently, the authors performed extensive experimental and theoretical studies on the bulk vapor flow, droplet dynamics and phase distribution of the dispersed flow (Wang, 1993; Wang and Mayinger, 1995). Based on the acquired knowledge, this paper discusses further our experiments on dispersed flow heat transfer in 90-degree circular bends.

EXPERIMENTAL APPARATUS AND PROCEDURE

Experiments on dispersed flow heat transfer were carried out in a refrigerant Freon-12 two-phase flow loop. Details of the test facilities can be found elsewhere (Wang, 1993; Wang and Mayinger, 1995). Here, only the layout of the test section and the relevant instrumentation are described. As shown in Figure 3, the test section consists of a vertical tube and a 90-degree vertical bend, Joule-heated by direct current. Through regulating the dryout location of the annular flow, dispersed flow was produced 2.5 m upstream the bend inlet, a length sufficient for flow development. The test section is made of stainless steel, having an inner diameter of 28.5 mm and a wall thickness of 2.6 mm. Two circular bends with different curvature radii (400 mm and 600 mm) were used. Due to bending, they have an ellipticity smaller than 4% and a maximum deviation in wall thickness of 4.6%.

Wall temperatures were measured by NiCr-Ni thermocouples of 0.5 mm diameter, spot welded on the outside surface of the tube (see Fig. 3 for distribution). Inner surface temperatures were then inferred by the Fourier conduction equation. Local vapor temperatures were estimated from the signals of two movable thermocouples installed in the flow channel as a first approximation. The transient effect of the droplet interference on the signals was filtered off prior to the evaluation. Early calibration of this simple measuring technique with a differential suction probe (Lautenschlager, 1988) indicated that it provided also satisfactory results, especially in the high quality region. Based on the measurement of the uniform wall heat flux and the local vapor temperature, apparent heat transfer coefficients were deduced. Here, difference should be noticed between the "apparent" and "true" heat transfer coefficients, which is subjected to changes in local geometry, changes in temperature/geometry-dependent resistivity, axial and circumferential conduction. The first two factors have been estimated to introduce about 5% higher volume heating at the inner and 5% lower

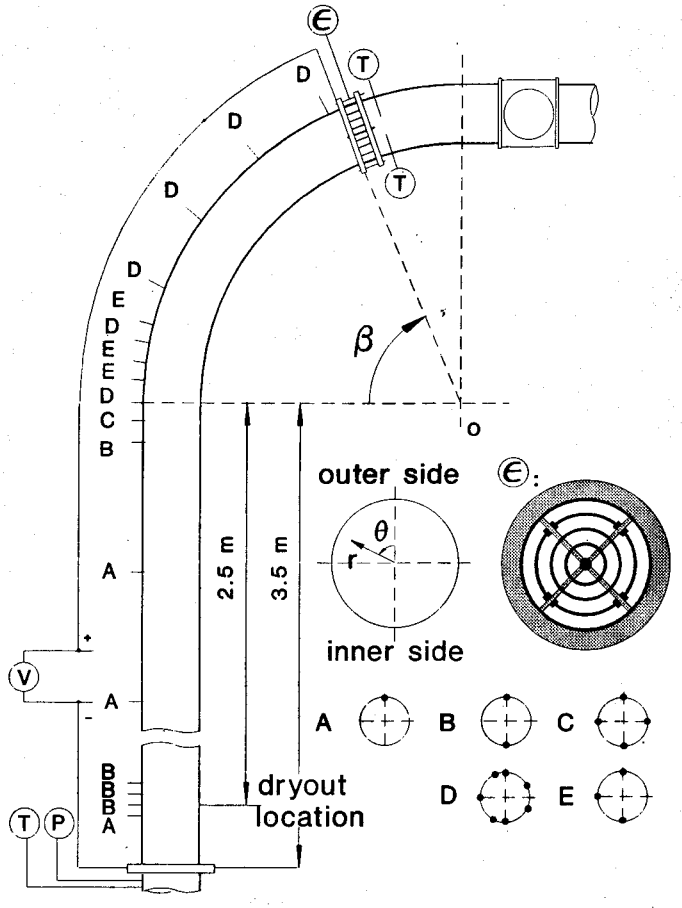

FIGURE 3 Layout of the test section.

volume heating at the outer side of the bend. The last factor, predominantly the circumferential conduction, produces an opposite effect, i.e. the true local heat flux at the outside is larger, and at the inside is smaller than the apparent one. Sample evaluations (Lautenschlager, 1988) showed that this effect may bring about 10 to 15% difference between the apparent and true local heat flux.

In order to study the effect of flow structure on heat transfer, a specially developed impedance probe was used to measure the local liquid fraction. By changing the probe angular positions, phase distribution along the bend was obtained. Figure 3 shows a sketch of the impedance probe. It is composed of five separate capacitors, electrically isolated and supported by an epoxide frame. Supplied with high-frequency voltage, these capacitors convey local dielectric constant signals, which can be transformed into liquid fractions under specific flow regimes. For dispersed flow, liquid fraction can be well determined from the dielectric constants of two-phase mixture, pure liquid and pure gas by the Maxwell correlation (Cimorelli and Evangelisti, 1967). An error

analysis of this measuring technique indicated (Wang, 1993) that the impedance probe gives a good indication of liquid fraction even if there is a thin film forming on one of the electrodes due to the droplet impingement. For example, the relative error for liquid fraction accounts for about 9% if the liquid film occupies 10% of the total liquid.

The experiments covered a wide range of operational parameters: mass flow rate G, 400–2000 kg/m^{2}s; wall heat flux $\dot{q}_w$, 20–70 kW/m^2, bend/tube radius ratio (curvature ratio) R_c/R, 28, 42; reduced pressure P/P_{cr}, 0.23–0.70.

RESULTS AND DISCUSSION

Heat Transfer Patterns

In circular bends, intensive interactions between droplet-vapor, droplet-wall and vapor-wall (Wang, 1993; Wang and Mayinger, 1995) result in complicated heat transfer patterns, which can be essentially classified into two different patterns, namely, heat transfer without and with rewetting. The terminology "rewetting" means here the re-establishment of continuous liquid contact with the hot wall, when the wall is cooled below the Leidenfrost temperature.

Figure 4 presents distributions of wall temperature and heat transfer coefficient under non-rewetting pattern. For comparison, computational results of bulk vapor convection (Wang, 1993) are included. As seen from the figure, the bend wall maintains a high degree of superheating, which prevents droplets from stable contact with the wall. Shortly after the bend inlet, heat transfer is found to be improved at the outer wall and slightly deteriorated at the inner wall. The difference reaches a maximum at about 20- to 30-degree angular position, where the heat transfer coefficient at the outside is about 2 to 3 times larger than that at the inside. In the middle part of the bend, there is a slight improvement of heat transfer at the inside. In the later part, a fully developed heat transfer pattern is gradually formed: temperature difference between the inner and outer side is nearly constant, similar to that observed by Cumo *et al.* (1972) in coil experiments.

To clarify the intrinsic mechanisms under non-rewetting status, vapor convection, droplet deposition process and phase distribution are studied for the same condition. According to the heat transfer results of bulk vapor flow in Figure 4b, vapor convection makes only a weak contribution to the heat transfer improvement in the early part of the bend. Therefore, the role of droplet dynamics should be particularly considered. As illustrated in Figure 5a, the centrifugally induced phase separation develops immediately downstream the bend inlet, which changes the local heat transfer condition at the outer and inner wall correspondingly. In addition, droplet trajectory analysis of Wang (1993) indicates that the outward moving droplets possess high deposition velocities, sufficient for transient contact with the wall (see Figs. 5b, 2). Through droplet impact, breakup and evaporation on the wall, local heat transfer is significantly improved. Here, it is interesting to find that the position of the maximum deposition velocity agrees exactly with that of the maximum heat transfer coefficient at the outer wall. This coincidence confirms again the dominant contribution of droplet-wall interactions to the heat transfer augmentation. In the middle part of the bend where the secondary

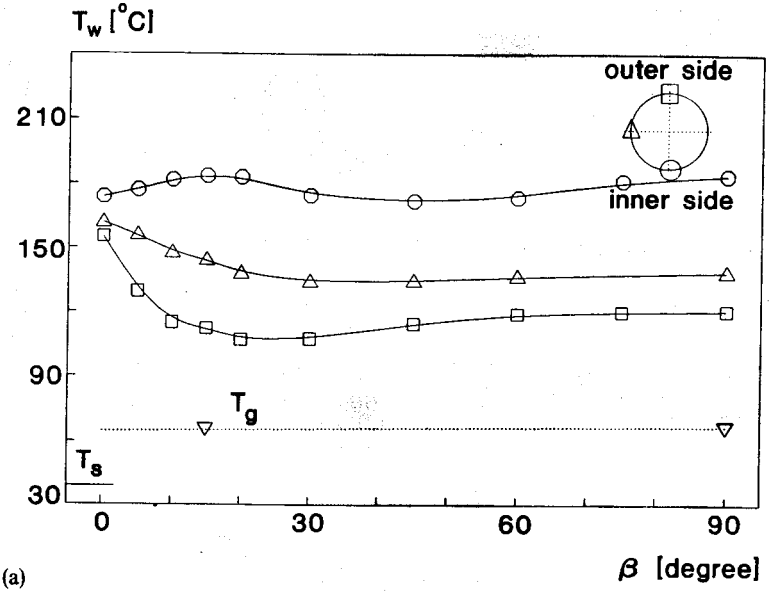

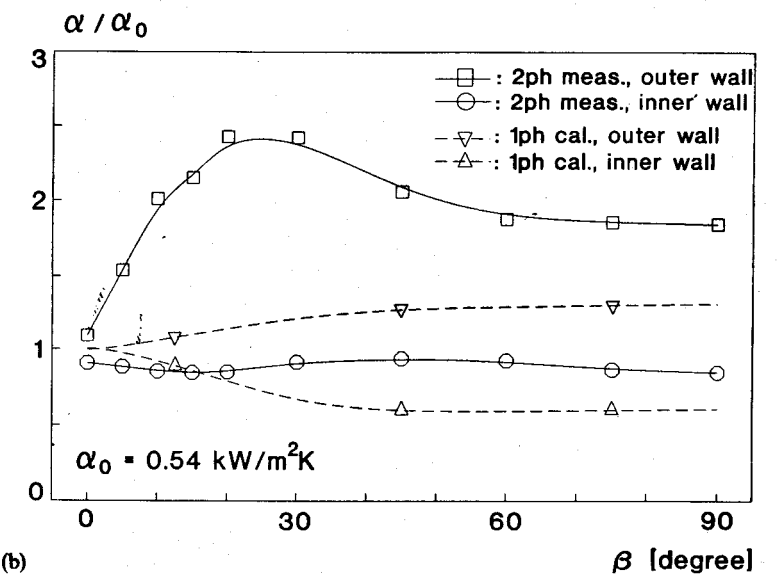

FIGURE 4 Heat transfer measurement under non-rewetting pattern: $R_c/R = 42$, $G = 680\,\mathrm{kg/m^2}$, $\dot{q}_w = 50\,\mathrm{kW/m^2}$, $P/P_{cr} = 0.23$, $x_0 = 0.75$, $d_0 = 280\,\mu\mathrm{m}$, (a) distribution of wall temperature (b) distribution of heat transfer coefficient.

flow attains maximum (see Fig. 1), some small droplets are transported to the inner side (see Figs. 2,5a), in which they act as local heat sinks and improve the local heat transfer slightly. The importance of droplet dynamics decreases in the later part of the bend as droplets evaporate and the deposition rate decreases.

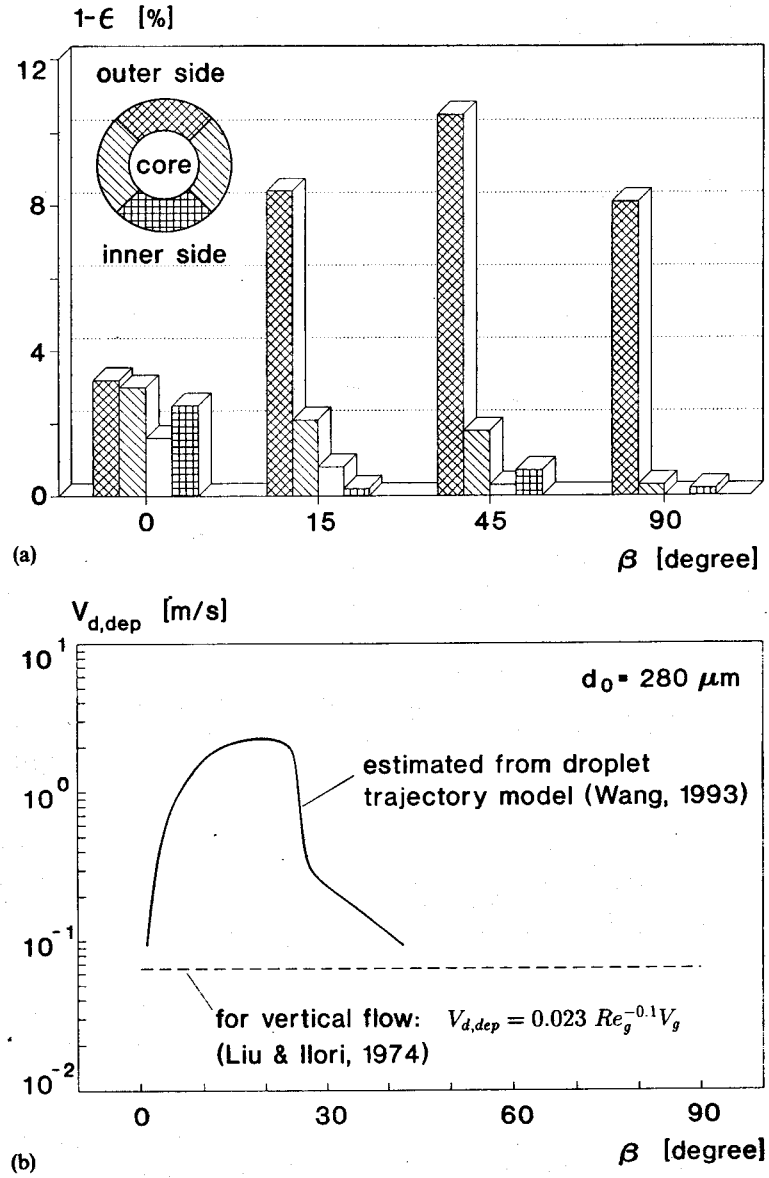

FIGURE 5 Evaluation of dispersed flow dynamics under the non-rewetting condition of Figure 4. (a) measurement of phase distribution. (b) analysis of droplet deposition process.

Figure 6 shows the heat transfer measurement under rewetting pattern. Since the vapor phase is only slightly superheated in these conditions, heat transfer coefficient is calculated based on the saturation temperature. It can been seen from the figure that within the first 10-degree bend angle, the outer wall is quenched quickly from a high

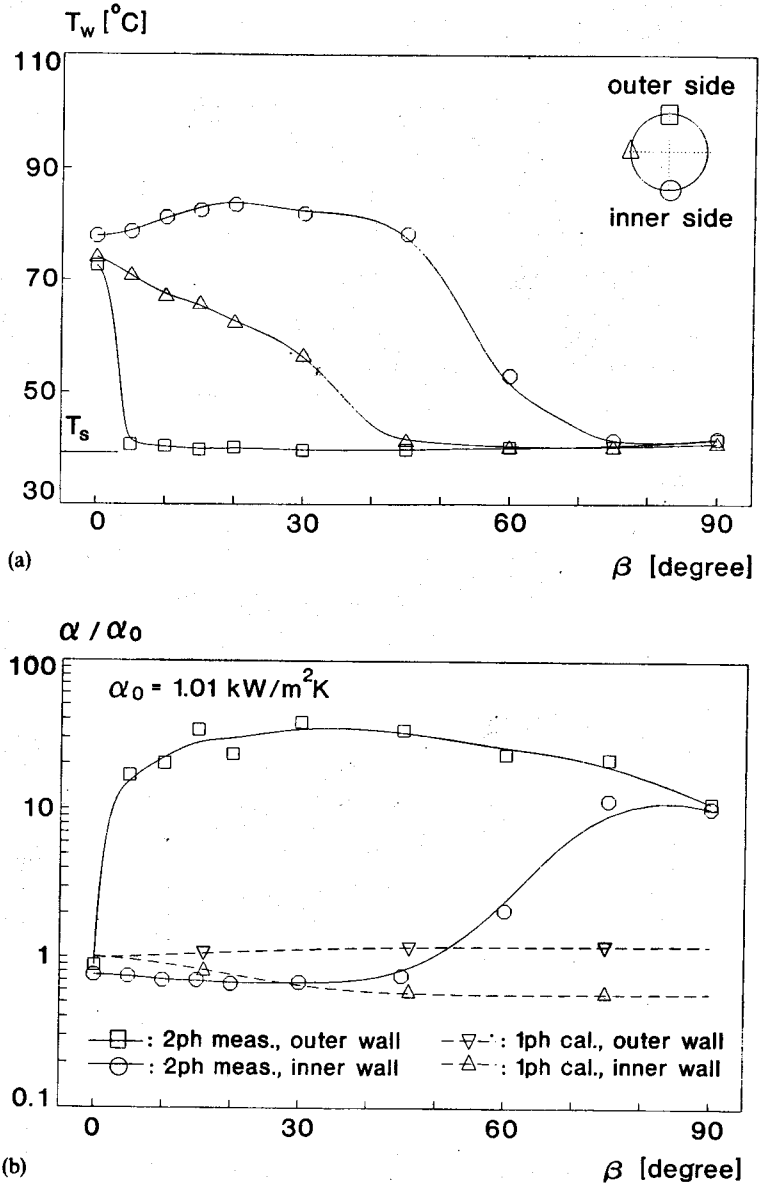

FIGURE 6 Heat transfer measurement under rewetting pattern: $R_c/R = 42$, $G = 1240\,\mathrm{kg/m^2}$, $\dot{q}_w = 30\,\mathrm{kW/m^2}$, $P/P_{cr} = 0.23$, $x_0 = 0.78$, $d_0 = 130\,\mu\mathrm{m}$, (a) distribution of wall temperature (b) distribution of heat transfer coefficient.

superheating state down to a value near the saturation temperature, resulting in an order-of-magnitude increase of heat transfer coefficient. This rewetting state keeps almost stable for the rest part of the outer bend. Heat transfer at the inside of the bend changes similarly as that under non-rewetting pattern up to about 40-degree, where the

inner wall temperature is found to decrease significantly. Beginning from the middle of the bend, temperature readings at the side and inner wall indicate that rewetting spreads along the tube circumference from the outer to the inner wall, leading to a total heat transfer augmentation in the bend.

Comparing the measurements without and with rewetting in Figures 4 and 6, it is apparent that rewetting brings about entirely different heat transfer performance. To analyze the relevent mechanism, fluid-dynamic aspects of the flow under rewetting are examined in Figure 7. As seen in Figure 7a, phase separation results in liquid accumulation at the outer and deficiency at the inner region in the first half of the bend. More important is the fact that droplets deposit on the outer wall at very high rates, as indicated in Figure 7b. By intensive droplet impingement, the outer wall may be cooled below the Leidenfrost temperature. One this threshold is exceeded, droplets can maintain stable contact with the outer wall, where they easily link together and form a continuous liquid film. A mode of convective film evaporation is therefore established. Further downstream, Figure 7a clearly confirms the inward transportation of liquid film induced by the secondary vapor flow and the gravity.

Parametric Effects

In view of the analysis in the previous section, dispersed flow heat transfer may be influenced by different parameters. Here, we will discuss the effects of the four most important parameters: mass flow rate, wall heat flux, system pressure and curvature ratio.

Figure 8 illustrates the effect of mass flow rate on the temperature distributions at the outer wall of the bend. It can be seen that for given wall heat flux, system presure and curvature ratio, increase in mass flow rate leads to heat transfer augmentation, obviously due to increased droplet-wall interactions and vapor convection. If the mass flow rate is high enough, rewetting on the wall may be initiated. For the mass flow rate of 2000 kg/m^2s, rewetting appears even within the first 5 degrees from the bend inlet. This is clearly attributed to the intensive droplet deposition process, which becomes dominant at higher mass flow rate. The reason is as follows. In film boiling, a higher mass flow rate corresponds to a higher fluid velocity, higher liquid fraction, lower wall superheating and smaller droplet size. According to the previous analysis, the first three factors are more important. As a function of the square of the mean velocity, the centrifugal forces produce a higher deposition rate at higher mass flow rate, which can easily change the superheating boundary condition and bring about the onset of rewetting.

Figure 9 shows the wall temperature measurement at different heat fluxes while maintaining mass flow rate, curvature ratio and system pressure constant. As seen from the figure, increase in heat flux reduces the rewetting region and therefore the total heat transfer rate. When heat flux is elevated to 50 kW/m^2, heat transfer pattern changes from rewetting to non-rewetting state. This implies that under a certain droplet deposition process, there exists a critical wall heat flux, beyond which a continuous accumulation of liquid on the wall is prevented by the rapid evaporation of droplets and the thermal repelling forces near the hot wall. It is also interesting to find that at non-rewetting state, heat transfer pattern exhibits almost the same features at different wall heat fluxes: wall temperature decreases continuously in the first 30 degrees from

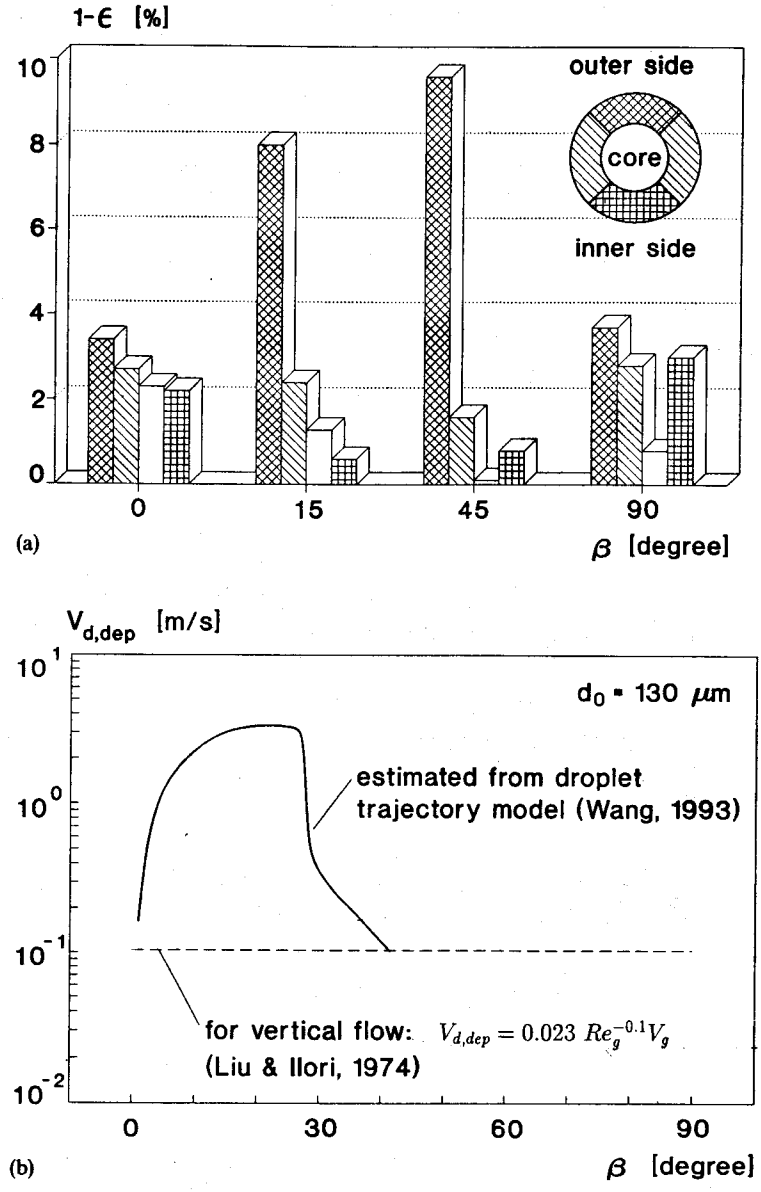

FIGURE 7 Evaluation of dispersed flow dynamics under the rewetting condition of Figure 6. (a) measurement of phase distribution. (b) analysis of droplet deposition process.

the bend inlet because of the droplet impingement, and after then increases gradually as droplet-wall interactions reduce.

Figure 10 demonstrates the influence of system pressure on heat transfer. It can been seen in the figure that the heat transfer behavior at high pressures differs greatly from

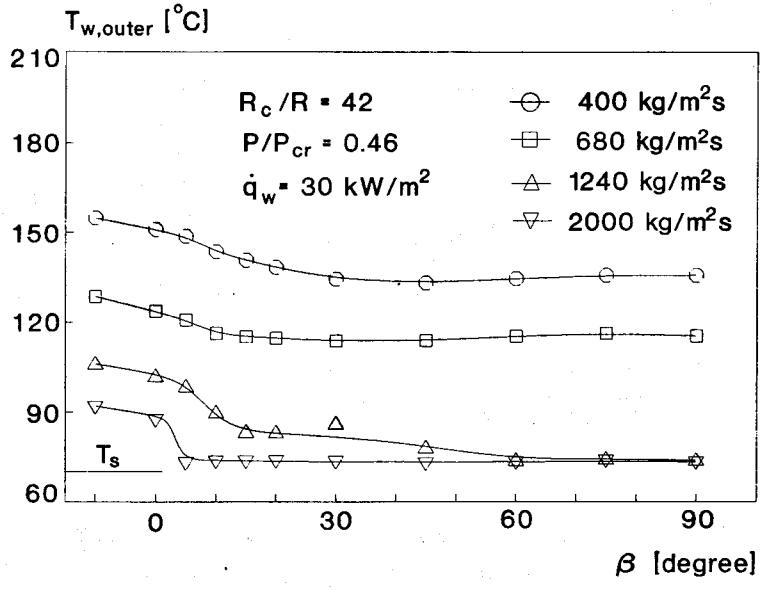

FIGURE 8 Influence of mass flow rate on heat transfer.

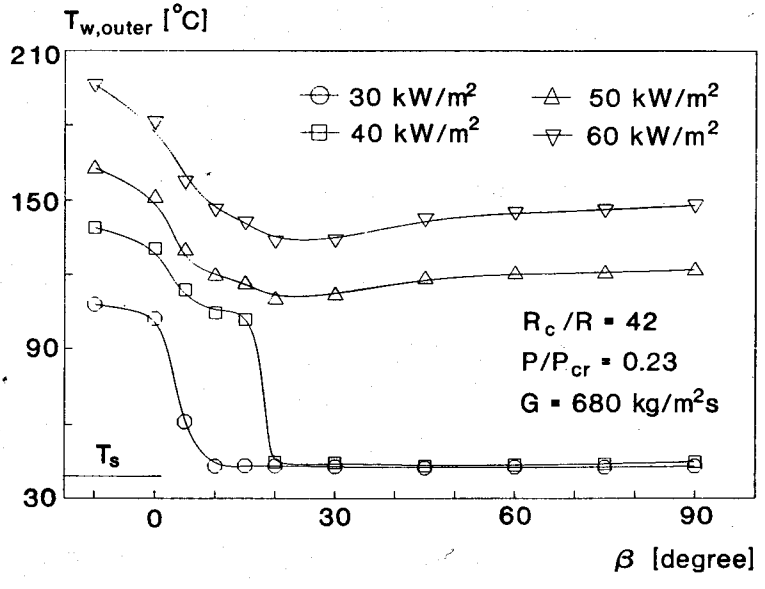

FIGURE 9 Influence of wall heat flux on heat transfer.

that at low pressure. Under the same mass flow rate, wall heat flux and curvature ratio, heat transfer is generally poor at high pressures and rewetting seems much difficult to take place. In addition, heat transfer features connected with curvature are minimized at high pressures and the wall temperature distributions look similar to those under

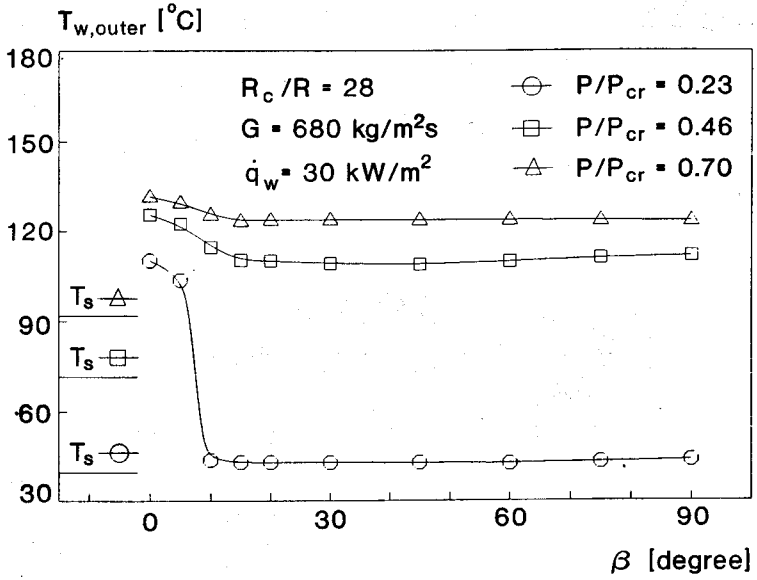

FIGURE 10 Influence of system pressure on heat transfer.

film boiling in vertical channels. Such effect of pressure can be mainly attributed to the density changes of the fluids in two aspects. Firstly, increase in pressure decreases the liquid density and increases the vapor density, which reduce the centrifugal forces and droplet-wall interactions. Secondly, with the same mass flow rate, mean velocity decreases with the decrease in the density difference. Therefore the droplet deposition velocity, which is governed by the mean velocity, decreases correspondingly. These two factors weaken the effect of droplet dynamics and thus the heat transfer in the bend.

Figure 11 presents the effect of curvature ratio on the wall temperature distributions. Comparing the measurements from two different bends, it can be found in the figure that in the first 30 degrees from the bend inlet, there is a better heat transfer at the outer wall, a poorer heat transfer at the inner wall of the small-radius bend. This reveals the dominant effect of phase separation on heat transfer at the early part of the bend. In the small-radius bend, the centrifugal forces are larger and can produce stronger droplet-wall interactions at the outer wall. In the middle of the bend, however, such interactions decrease to a great extent and hence heat transfer at the outer wall of both two bends deteriorates. Here it is interesting to observe the effect of secondary flow, which attains maximum in this region (Wang and Mayinger, 1995). Through the secondary flow transportation, more coolant from the outside enters the inner region of the small-radius bend, leading to a better local heat transfer. In the later part of the inner bend, this effect decreases gradually as the secondary flow velocity reduces and the heat transfer at the outside further deteriorates.

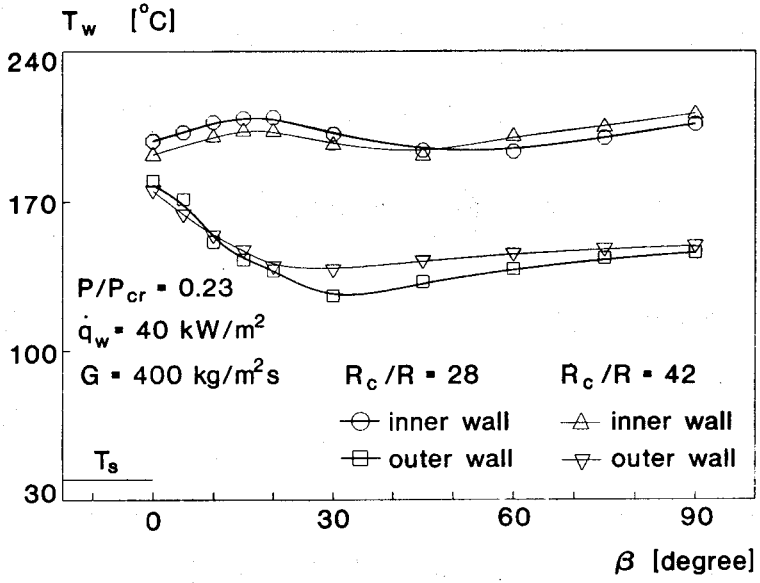

FIGURE 11 Influence of curvature ratio on heat transfer.

Criterion of Heat Transfer Pattern

Using the present experimental data, it is possible to develop a criterion for identification of the heat transfer pattern, which will assist system design or safety analysis in a number of industrial situations. This criterion should clearly reflect the controlling process involved and should be potentially applicable also for other fluids. Based on these considerations, dimensional analysis is applied to study the onset condition of rewetting.

It has been revealed in the previous sections that the regime without rewetting is actually the heat flux dominant regime, where wall heat flux is large enough to sustain a high superheating boundary condition under a certain range of droplet deposition flux. On the contrary, the regime with rewetting is the deposition dominant regime, where the droplet deposition flux is sufficiently high to quench the wall below the Leidenfrost limit within a certain range of wall heat flux. Obviously, the demarcation between the rewetting and non-rewetting regimes is determined by evaporation related parameters such as wall heat flux, latent heat of the fluid, deposition related parameters such as mass flow rate of liquid, vapor quality, curvature radius, densities of both phases, and the parameters governing the wetting behavior such as surface tension and liquid viscosity. Combining these parameters into dimensionless forms, five groups

$$\frac{\dot{q}_w}{Gh_{fg}}, \quad \frac{\rho_g}{\rho_l}, \quad \frac{G(1-x)D}{\mu_l}, \quad \frac{R_c}{D}, \quad \frac{G^2 D}{\sigma \rho_l}$$

are arrived, which are believed important in characterizing the aforementioned controlling processes. Using the test points near the transition of heat transfer pattern as

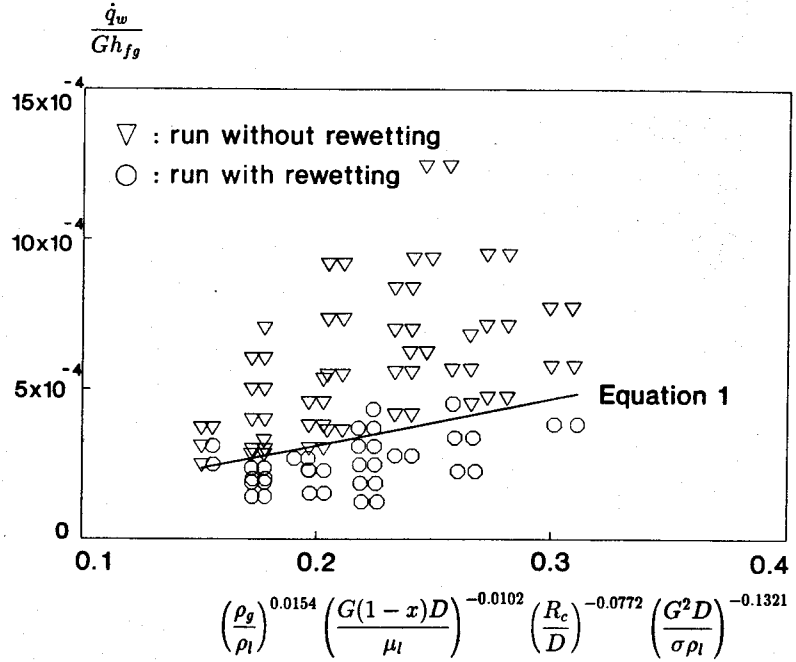

FIGURE 12 Transition of heat transfer pattern.

the regression data base, the following transition correlation was established

$$\frac{\dot{q}_w}{Gh_{fg}} = 1.567 \times 10^{-3}\left(\frac{\rho_g}{\rho_l}\right)^{0.0154}\left(\frac{G(1-x)D}{\mu_l}\right)^{-0.0102}\left(\frac{R_c}{D}\right)^{-0.0772}\left(\frac{G^2D}{\sigma\rho_l}\right)^{-0.1321} \quad (1)$$

Taking the dimensionless parameter in the LHS of the equation as the y-coordinate and the combination of the dimensionless parameters in the RHS of the equation as the x-coordinate, this correlation is displayed together with 96 test runs of our experiment in Figure 12. It can been clearly seen that all the heat flux controlled non-rewetting points lie above the transition line, whereas almost all the deposition controlled rewetting points lie below the transition line. In addition, parametric effects on the change of heat transfer pattern can be intuitively observed in the figure. Therefore, Equation 1 is a reliable criterion of the heat transfer pattern for Freon 12. Further study is needed to examine its applicability to other working fluids with the same channel material.

CONCLUSIONS

Experimental results on dispersed flow heat transfer in circular bends have been presented over a wide parametric range. The main conclusions are given as follows.

1. Dispersed flow heat transfer in bends can be essentially classified into two different patterns, i.e. heat transfer without and with rewetting. The occurrence of

a specific pattern depends jointly on the wall heat flux condition and the droplet deposition condition.

2. Non-rewetting heat transfer appears at high heat fluxes, small to median mass flow rates, and frequency at median to high system pressures. In this pattern film boiling maintains. Heat transfer is improved by the centrifugally induced droplet wall interactions and the secondary flow transportation.
3. Rewetting heat transfer occurs at small to median heat fluxes, median to high mass flow rates and mostly at low pressures. Due to the intensive droplet impingement, rewetting appears firstly on the outer wall. Then, it spreads gradually along the circumference to the inner wall by the vapor shear and the gravity. Through convective film evaporation, an order-of-magnitude increase of heat transfer coefficient is observed.
4. An empirical criterion is developed to identify the heat transfer pattern in the bend. It has a satisfactory accuracy for our Freon-12 data. Its applicability to other working fluids needs to be further examined.

NOMENCLATURE

d	Droplet diameter, m(μm)
D	Tube diameter, m
G	Mass flow rate, kg/m^{2}s
h_{fg}	Latent heat, J/kg
P	Pressure, Pa (bar)
$\dot{q}$	Heat flux, W/m^2
r	Radial coordinate, m
R	Tube radius, m
R_c	Bend radius, m
Re_g	Reynolds number of vapor phase, $\rho_g V_g D/\mu_g$
T	Temperature, K(°C)
V	Velocity, m/s
$V_{d,dep}$	Droplet deposition velocity, m/s
x	Vapor quality

Greek Symbols

α	Heat transfer coefficient, W/m^{2}K
β	Bend angle, degree
ε	Void fraction
θ	Polar coordinate
μ	Dynamic viscosity, kg/ms
ρ	Density, kg/m^3
σ	Surface tension, N/m

Subscripts

cr	Critical
d	Droplet

g	Vapor
l	Liquid
s	Saturation
w	Wall
0	Mean parameter at bend inlet

REFERENCES

Cimorelli, L., and Evangelisti, R. The Application of the Capacitance Method for Void Fraction Measurement in the Bulk Boiling Conditions, *Int. J. Heat Mass Transfer*, **10**, 277 (1967).

Cumo, M., Farello, G. E., and Ferrari, G. The Influence of Curvature in Post Dry-Out Heat Transfer, *Int. J. Heat Mass Transfer*, **15**, 2045 (1972).

Lautenschlager, G. Wärmeübergang in Krümmern bei Sprühkühlung, *Dissertation*, Technische Universität München (1988).

Liu, B. Y. H., and Ilori, T. A. Aerosol Deposition in Turbulent Pipe Flow, *Environmental Sci. and Tech.*, **8**, 351 (1974).

Mayinger, F. *Strömung and Wärmeübertragung in Gas-Flüssigkeits-Gemischen*, Springer Verlag, Wien (1982).

Styrikovich, M. A., Polonsky, V. S., and Reshetov, V. V. Experimental Investigation of the Critical Heat Flux and Post-Dryout Temperature Regime of Helical Coils, *Int. J. Heat Mass Transfer*, **27**, 1245 (1984).

Wang, M. J. *Phase Distribution, Secondary Flow and Heat Transfer of Dispersed Flow in Circular Bends*, Verlag Shaker, Aachen (1993)

Wang, M. J., and Mayinger, F. Post-Dryout Dispersed Flow in Circular Bends, *Int. J. Multiphase Flow* **21**, 437 (1995).